Low energy proton-proton scattering in effective field theory

Shung-ichi Ando,[*] Jae Won Shin, Chang Ho Hyun, and Seung-Woo Hong
Department of Physics, Sungkyunkwan University, Suwon 440-746, Korea
(Received 7 May 2007; revised manuscript received 4 October 2007; published 10 December 2007)

Low energy proton-proton scattering is studied in pionless effective field theory. Employing the dimensional regularization and $\overline{\rm MS}$ and power divergence subtraction schemes for loop calculation, we calculate the scattering amplitude in the $^1S_0$ channel up to the next-to-next-to leading order and fix low-energy constants that appear in the amplitude by effective range parameters. We study the regularization scheme and scale dependence in the separation of the Coulomb interaction from the scattering length and effective range for the S-wave proton-proton scattering.

DOI: 10.1103/PhysRevC.76.064001 PACS number(s): 11.10.Gh, 13.75.Cs, 25.40.Cm

I. INTRODUCTION

Effective field theories (EFTs), which provide us a systematic perturbative scheme and a model-independent calculation method, have become a popular method to study hadronic reactions with and without external probes at low and intermediate energies. (See, e.g., Refs. [1–5] for reviews.) At very low energies, the Coulomb interaction becomes essential for the study of reactions involving charged particles. The first consideration of the Coulomb interaction in a pionless EFT was done by Kong and Ravndal (KR) for low energy S-wave proton-proton (pp) scattering [6,7]. They calculated the pp scattering amplitude up to next-to leading order (NLO). For loop calculations, they employed dimensional regularization with the minimum subtraction (MS) scheme and so-called power divergence subtraction (PDS) scheme suggested by Kaplan, Savage, and Wise [8,9]. Then KR estimated a scattering length $a(\mu)$ for the pp scattering after separating off the Coulomb correction where μ is the scale for dimensional regularization. The leading order (LO) result of $a(\mu)$ was almost infinite at $\mu = m_\pi$ where m_π is the pion mass [6]. In addition, the LO $a(\mu)$ was highly dependent on the value of μ. Including the NLO correction, they obtained $a(\mu = m_\pi) = -29.9$ fm [7] which is comparable to the value of the scattering length a_{np} in the np channel, $a_{np} = -23.748 \pm 0.009$ fm.[1]

The value of $a(\mu)$ deduced after separating the Coulomb and strong interactions is particularly important in the study of isospin breaking effects in the S-wave NN interaction [11,12]. The accurate value of a_{np} is well known as quoted above, while the values of the scattering length in the nn channel (a_{nn}) and in the pp channel (a_{pp}) still have considerable uncertainties.

There exists no direct nn scattering experiment because of the lack of a *free* neutron target. The values of a_{nn} have been deduced from the experimental data of $\pi^- d \to nn\gamma$ and $nd \to nnp$ reactions. Recent publications suggest $a_{nn} = -18.50 \pm 0.05(\text{stat.}) \pm 0.44(\text{syst.}) \pm 0.30(\text{th.})$ fm from the $\pi^- d \to nn\gamma$ process [13], and $a_{nn} = -18.7 \pm 0.6$ fm [14], -16.06 ± 0.35 fm [15], and -16.5 ± 0.9 fm [16] from the $nd \to nnp$ process. As seen, the values of a_{nn} have significant errors compared to that of a_{np}, and the center values do not seem to converge yet.[2]

For the pp channel, a very accurate value of the scattering length $a_C = -7.828 \pm 0.008$ fm [19] and $a_C = -7.8149 \pm 0.0029$ fm [20] are available from the low energy pp scattering data. It contains, however, contributions from both strong and electromagnetic interactions, and thus we need to disentangle the strong interaction from the electromagnetic interaction. It was pointed out in potential model calculations that there is a considerable model dependence in deducing the value of the strong scattering length a_{pp} from a_C [19,21]. Some literature shows $a_{pp} = -17.1 \pm 0.2$ fm [19], while a heavy-baryon chiral perturbation theory results in $a_{pp} = -17.51 \sim -16.96$ fm [22] with uncertainties slightly larger than those from the potential models.

In this work, we employ the pionless EFT [23] including the Coulomb interaction between two protons [6,7] and calculate the pp scattering amplitude with the strong NN interactions up to next-to-next-to leading order (NNLO). Our main motivation of this study is to see how the value of strong scattering length $a(\mu = m_\pi) = -29.9$ fm obtained by KR from NLO calculations may be improved by the inclusion of a higher order correction. We find that the NNLO corrections turn out to be quite small, but there is a considerable dependence of the scattering length $a(\mu)$ on the renormalization schemes and the scale parameter μ.

This paper is organized as follows. In Sec. II, we briefly review the effective range formalism for the pp scattering. In Sec. III, the pionless strong effective Lagrangian up to NNLO is introduced. In Sec. IV, we calculate the S-wave pp scattering amplitude up to NNLO. In Sec. V, we discuss the regularization method and renormalization schemes employed in this work. We renormalize low energy constants (LECs) that appear in the strong NN interaction up to NNLO by effective range parameters employing MS-bar ($\overline{\rm MS}$) and PDS schemes and obtain numerical results for the strong scattering length $a(\mu)$ and strong effective range $r(\mu)$. Discussion and

[*]sando@color.skku.ac.kr

[1]See, e.g., Table VIII in Ref. [10].

[2]Recently, there were proposals to determine the value of a_{nn} more precisely by employing a formalism of EFT, from the $\pi^- d \to nn\gamma$ reaction [17] and neutron-neutron fusion, $nn \to de^-\bar{\nu}_e$ [18].

conclusions are given in Sec. VI. In Appendix A, we show detailed expressions of the amplitudes in NNLO. Detailed calculations of the loop functions employing the dimensional regularization and $\overline{\rm MS}$ and PDS schemes are given in Appendix B.

II. PROTON-PROTON SCATTERING IN EFFECTIVE RANGE THEORY

The amplitude of the pp scattering can be decomposed as [24]

$$T = T_C + T_{\rm SC}, \tag{1}$$

where T_C is the pure Coulomb part and $T_{\rm SC}$ is the "modified" strong amplitude whose S-wave channel we calculate up to NNLO in pionless EFT below.

The incoming and outgoing scattering states $|\Psi_{\vec p}^{(\pm)}\rangle$ with the potential $\hat V = \hat V_C + \hat V_S$, where $\hat V_C$ and $\hat V_S$ are the Coulomb and strong potentials, respectively, are represented in terms of the Coulomb states $|\psi_{\vec p}^{(\pm)}\rangle$ as

$$|\Psi_{\vec p}^{(\pm)}\rangle = \sum_{n=0}^{\infty}\left(\hat G_C^{(\pm)}\hat V_S\right)^n|\psi_{\vec p}^{(\pm)}\rangle, \tag{2}$$

where $\hat G_C^{(\pm)}$ is the incoming and outgoing Green's function

$$\hat G_C^{(\pm)}(E) = \frac{1}{E-\hat H_0-\hat V_C \pm i\epsilon}. \tag{3}$$

Here $\hat H_0 = \hat p^2/M$ is the free Hamiltonian of two protons and $V_C = e^2/(4\pi r)$ is the repulsive Coulomb potential. The Coulomb state $|\psi_{\vec p}^{(\pm)}\rangle$ is obtained by solving the Schrödinger equation $(\hat H - E)|\psi_{\vec p}^{(\pm)}\rangle = 0$ with $\hat H = \hat H_0 + \hat V_C$, and thus one has

$$|\psi_{\vec p}^{(\pm)}\rangle = \left[1 + \hat G_C^{(\pm)}\hat V_C\right]|\vec p\rangle, \tag{4}$$

where $|\vec p\rangle$ is the free wave state. The normalization of $|\psi_{\vec p}^{(\pm)}\rangle$ is such that $\langle\psi_{\vec p}^{(\pm)}|\psi_{\vec q}^{(\pm)}\rangle = (2\pi)^3\delta^{(3)}(\vec p-\vec q)$. The amplitude $T_{\rm SC}$ is thus obtained by

$$T_{\rm SC}(\vec p\,', \vec p) = \sum_{n=0}^{\infty}\langle\psi_{\vec p\,'}^{(-)}|\hat V_S(\hat G_C^{(+)}\hat V_S)^n|\psi_{\vec p}^{(+)}\rangle. \tag{5}$$

For $l=0$ state, one has the amplitude

$$T_{\rm SC}^{l=0} = -\frac{4\pi}{M}\frac{e^{2i\sigma_0}}{p\cot\delta_0 - ip}, \tag{6}$$

where σ_l is the Coulomb phase shift $\sigma_l = \arg\Gamma(1+l+i\eta)$ with $\eta = \alpha M/(2p)$. In the effective range expansion with the Coulomb interaction, the modified strong phase shift δ_l for $l=0$ in low energy pp scattering is represented by effective range parameters [25]:

$$C_\eta^2 p\cot\delta_0 + \alpha M h(\eta) = -\frac{1}{a_C} + \frac{1}{2}r_0p^2 - Pr_0^3p^4 + \cdots, \tag{7}$$

where $C_\eta^2 = 2\pi\eta/(e^{2\pi\eta}-1)$ and

$$h(\eta) = {\rm Re}\,\psi(i\eta) - \ln\eta. \tag{8}$$

The ψ function is the logarithmic derivative of the Γ function and ${\rm Re}\,\psi(i\eta) = \eta^2\sum_{\nu=1}^{\infty}\frac{1}{\nu(\nu^2+\eta^2)} - C_E$; C_E is the Euler's constant, $C_E = 0.577\,215\cdots$. Effective range parameters a_C, r_0, and P, are the modified scattering length, effective range, and effective volume, respectively.

III. EFFECTIVE LAGRANGIAN

Pionless effective Lagrangian for strong S-wave NN interaction up to NNLO reads [23,26]

$$\begin{aligned}\mathcal{L} = {}& N^\dagger\left(iD_0 + \frac{\vec D^2}{2m_N}\right)N - C_0\left[N^TP_a^{(^1S_0)}N\right]^\dagger N^TP_a^{(^1S_0)}N \\ &+ \frac{1}{2}C_2\left[N^TP_a^{(^1S_0)}\overleftrightarrow{D}^2N\right]^\dagger N^TP_a^{(^1S_0)}N + {\rm h.c.} \\ &- \frac{1}{2}C_4\left(N^TP_a^{(^1S_0)}\overleftrightarrow{D}^2N\right)^\dagger N^TP_a^{(^1S_0)}\overleftrightarrow{D}^2N \\ &- \frac{1}{4}\tilde C_4\left[\left(N^TP_a^{(^1S_0)}\overleftrightarrow{D}^4N\right)^\dagger N^TP_a^{(^1S_0)}N + {\rm h.c.}\right],\end{aligned} \tag{9}$$

where D_μ is the covariant derivative, $\overleftrightarrow{D} = \frac{1}{2}(\overrightarrow{D} - \overleftarrow{D})$, and $P_a^{(^1S_0)}$ is a projection operator for the two-nucleon $^1S_0$ states, $P_a^{(^1S_0)} = \frac{1}{\sqrt 8}\sigma_2\tau_2\tau_a$. Note that we retain two low energy constants, C_4 and $\tilde C_4$, in NNLO.

The strong NN potential is expanded in terms of small momentum as

$$\hat V_S = \hat V_0 + \hat V_2 + \hat V_4 + \cdots, \tag{10}$$

where $\hat V_0$, $\hat V_2$, $\hat V_4$ are LO, NLO, NNLO potential, respectively, and the matrix elements of them are obtained from the Lagrangian in Eq. (9) as

$$\langle\vec q|\hat V_0|\vec k\rangle = C_0, \tag{11}$$

$$\langle\vec q|\hat V_2|\vec k\rangle = \tfrac{1}{2}C_2(\vec q^{\,2} + \vec k^2), \tag{12}$$

$$\langle\vec q|\hat V_4|\vec k\rangle = \tfrac{1}{2}C_4\vec q^{\,2}\vec k^2 + \tfrac{1}{4}\tilde C_4(\vec q^{\,4} + \vec k^4), \tag{13}$$

where $|\vec q\rangle$ and $|\vec k\rangle$ are the intermediate free two-nucleon outgoing and incoming states, respectively; $2\vec q$ and $2\vec k$ are the relative momenta for the two protons.

In this work, we employ the standard counting rules of the strong NN interaction with the PDS scheme in Refs. [7,8]. (We will discuss the PDS scheme in detail later.) For the strong potential, the LO term C_0 is counted as Q^{-1} order, where Q denotes the small expansion parameter, and is summed up to an infinite order. The NLO (C_2) and NNLO (C_4, $\tilde C_4$) terms are counted as Q^2 and Q^4, respectively, and expanded perturbatively.[3] We treat the Coulomb interaction

[3]Note that by changing the LECs C_4 and $\tilde C_4$ in another linear combination, e.g., $C_4 = C_4' + \tilde C_4'$ and $\tilde C_4 = C_4' - \tilde C_4'$, one can easily see that the term proportional to $\tilde C_4'$ in Eq. (13) vanishes when $|\vec q| = |\vec k|$. The $\tilde C_4'$ term, the so-called off-shell term, is redundant and vanishes when the external legs of the potential go on mass-shell.

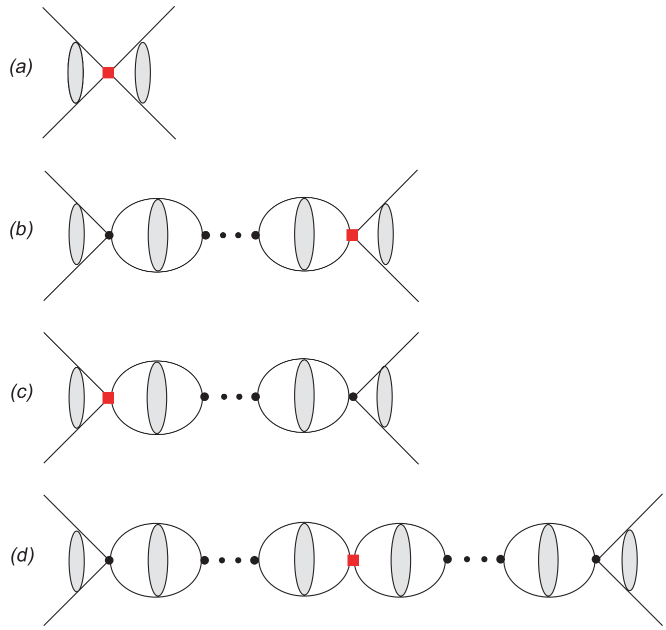

FIG. 1. (Color online) NLO diagrams for the S-wave pp scattering. Gray blobs denote the two-proton Coulomb Green's function $G_C^{(+)}$, and two nucleon contact vertices denote the strong potential: the (black) circle and the (red) square represent LO (C_0) and NLO (C_2) vertices, respectively. Small double dots stand for the summation of C_0 terms up to the infinite order.

nonperturbatively using Green's function $G_C^{(\pm)}$ in Eq. (3). We do not include higher order QED corrections such as the vacuum polarization effects reported in Ref. [27].

IV. AMPLITUDES

The amplitude $T_{SC}^{l=0}$ for the S-wave pp scattering can be written as

$$T_{SC}^{l=0} = T_{SC}^{(0)} + T_{SC}^{(2)} + T_{SC}^{(4)} + \cdots, \tag{14}$$

where $T_{SC}^{(0)}, T_{SC}^{(2)}, T_{SC}^{(4)}$ are LO, NLO, NNLO amplitudes, respectively. By inserting the strong LO potential $\hat{V}_0$ in Eq. (11) into the amplitude T_{SC} in Eq. (5), we obtain the LO amplitude $T_{SC}^{(0)}$ in terms of loop functions ψ_0 and J_0:

$$T_{SC}^{(0)} = \sum_{n=0}^{\infty} \langle \psi_{\vec{p}'}^{(-)} | \hat{V}_0 (\hat{G}_C^{(+)} \hat{V}_0)^n | \psi_{\vec{p}}^{(+)} \rangle = \frac{C_0 \psi_0^2(p)}{1 - C_0 J_0(p)}, \tag{15}$$

where

$$\psi_0(p) = \int \frac{d^3\vec{k}}{(2\pi)^3} \psi_{\vec{p}}^{(+)}(\vec{k}) = \int \frac{d^3\vec{k}}{(2\pi)^3} \psi_{\vec{p}}^{(-)*}(\vec{k}), \tag{16}$$

$$J_0(p) = \int \frac{d^3\vec{k}'}{(2\pi)^3} \frac{d^3\vec{q}}{(2\pi)^3} \langle \vec{q} | \hat{G}_C^{(+)} | \vec{k}' \rangle. \tag{17}$$

Detailed calculations for the functions ψ_0 and J_0 are given in Appendix B. $T_{SC}^{(0)}$ is the summation of the LO strong potential $\hat{V}_0$, that is, the C_0 terms summed up to the infinite order.

At NLO we have four diagrams shown in Fig. 1.[4] They are proportional to C_2 coming from $\hat{V}_2$, whereas the C_0 terms are summed up to the infinite order. The NLO amplitude is written in terms of the loop functions ψ_0, ψ_2, J_0, and J_2 as

$$T_{SC}^{(2,a-d)} = \frac{C_2 \psi_0}{(1 - C_0 J_0)^2} \left[\psi_2 + C_0 (\psi_0 J_2 - \psi_2 J_0) \right], \tag{18}$$

with

$$\psi_2(p) = \int \frac{d^3\vec{k}}{(2\pi)^3} \vec{k}^2 \psi_{\vec{p}}^{(+)}(\vec{k}) = \int \frac{d^3\vec{k}}{(2\pi)^3} \vec{k}^2 \psi_{\vec{p}}^{(-)*}(\vec{k}), \tag{19}$$

$$J_2(p) = \int \frac{d^3\vec{q}}{(2\pi)^3} \frac{d^3\vec{q}'}{(2\pi)^3} \vec{q}'^2 \langle \vec{q}' | \hat{G}_C^{(+)} | \vec{q} \rangle = \int \frac{d^3\vec{q}}{(2\pi)^3} \frac{d^3\vec{q}'}{(2\pi)^3} \times \langle \vec{q}' | \hat{G}_C^{(+)} | \vec{q} \rangle \vec{q}^2. \tag{20}$$

Details for ψ_2 and J_2 are given in Appendix B. The NLO amplitude $T_{SC}^{(2)}$ consists of one C_2 and a summation of the C_0 terms up to the infinite order. These LO and NLO amplitudes have already been obtained by KR in Ref. [7].

At NNLO, we have three sets of diagrams shown in Figs. 2–4. From the first and second sets of diagrams shown in Figs. 2 and 3, respectively, we see two NLO corrections to the amplitude, and thus the NNLO amplitudes obtained from the first and second sets of diagrams in Figs. 2 and 3 are proportional to C_2^2. The NNLO amplitudes corresponding to the diagrams in Fig. 2 can be written in terms of the functions ψ_0, ψ_2, J_0, and J_2; whereas to express the amplitudes for the diagrams in Fig. 3, we need a new function J_{22} given below. In the third set of diagrams shown in Fig. 4, we have one NNLO correction to the amplitude, and the NNLO amplitudes for the diagrams in Fig. 4 are proportional to C_4 or $\tilde{C}_4$. Explicit expressions of the NNLO amplitude from each of the diagrams are given in terms of ψ_i with $i = 0, 2, 4$ and J_j with $j = 0, 2, 22, 4$ in Appendix A.

Summing up the amplitudes obtained from the diagrams (a) to (h) in Figs. 2 and 3, we have

$$T_{SC}^{(4,a-h)} = \frac{C_2^2}{4(1 - C_0 J_0)^3} \left\{ \psi_0^2 J_{22} (1 - C_0 J_0) + \psi_2^2 J_0 (1 - C_0 J_0)^2 + 2\psi_0 \psi_2 J_2 \left(1 - C_0^2 J_0^2\right) + \psi_0^2 J_2 (C_0 J_2)(3 + C_0 J_0) \right\}, \tag{21}$$

where

$$J_{22} = \int \frac{d^3\vec{q}}{(2\pi)^3} \frac{d^3\vec{q}'}{(2\pi)^3} \vec{q}'^2 \langle \vec{q}' | \hat{G}_C^{(+)} | \vec{q} \rangle \vec{q}^2, \tag{22}$$

whose details are given in Appendix B.

Summing up the amplitudes for the diagrams (i) to (l) in

[4] Figures were prepared using the program JaxoDraw [28] provided by L. Theussl.

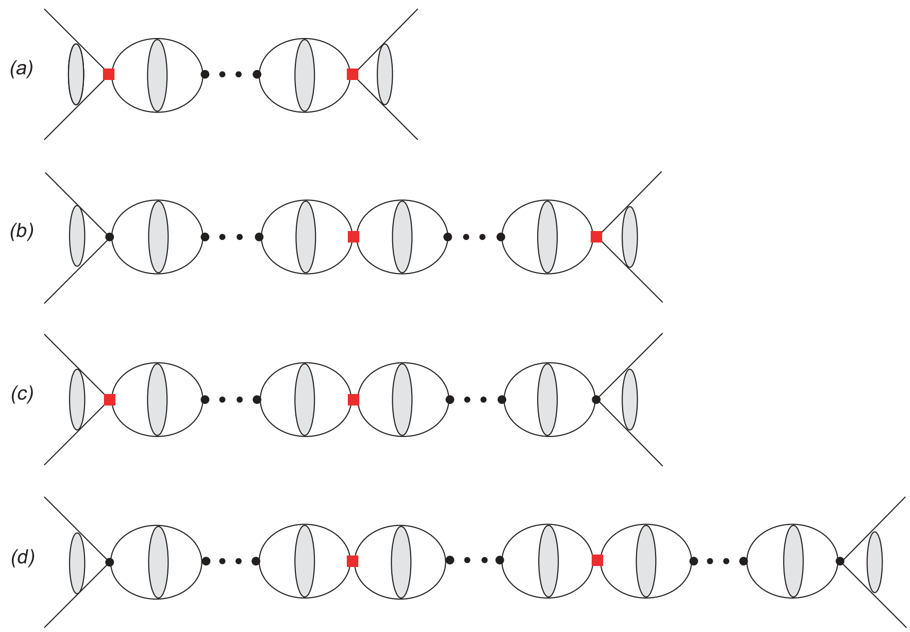

FIG. 2. (Color online) Set 1 of NNLO diagrams. See the caption of Fig. 1 for details.

Fig. 4 gives us

$$T_{\rm SC}^{(4,i-l)} = \frac{1}{2}\frac{C_4}{(1-C_0J_0)^2}\big[\psi_2^2(1-C_0J_0)^2 + 2\psi_0\psi_2C_0J_2(1-C_0J_0) + \psi_0^2C_0^2J_2^2\big] + \frac{1}{2}\frac{\tilde{C}_4}{(1-C_0J_0)^2}\left[\psi_4 + C_0(\psi_0J_4 - \psi_4J_0)\right]\psi_0, \tag{23}$$

where

$$\psi_4 = \int\frac{d^3\vec{k}}{(2\pi)^3}\psi_{\vec{p}}^{(-)*}(\vec{k})\vec{k}^4 = \int\frac{d^3\vec{k}}{(2\pi)^3}\vec{k}^4\psi_{\vec{p}}^{(+)}(\vec{k}), \tag{24}$$

$$J_4 = \int\frac{d^3\vec{q}}{(2\pi)^3}\frac{d^3\vec{q}\,'}{(2\pi)^3}\vec{q}\,'^4\langle\vec{q}\,'|\hat{G}_C^{(+)}|\vec{q}\rangle = \int\frac{d^3\vec{q}}{(2\pi)^3}\frac{d^3\vec{q}\,'}{(2\pi)^3}\langle\vec{q}\,'|\hat{G}_C^{(+)}|\vec{q}\rangle\vec{q}^{\,4}. \tag{25}$$

Calculations of ψ_4 and J_4 are given in Appendix B.

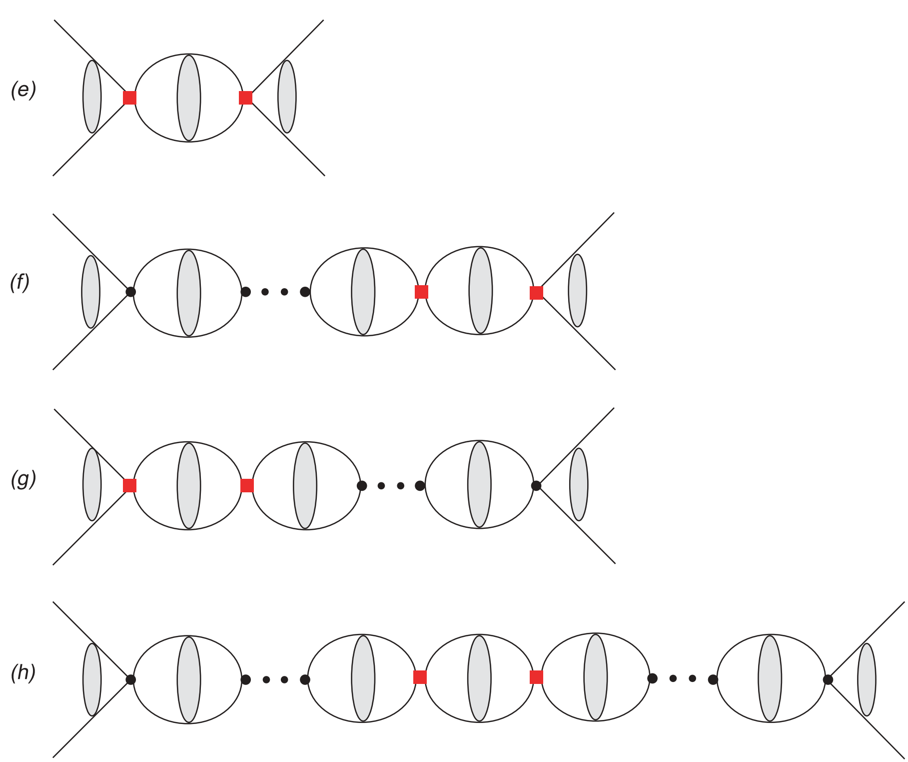

FIG. 3. (Color online) Set 2 of NNLO diagrams. See the caption of Fig. 1 for details.

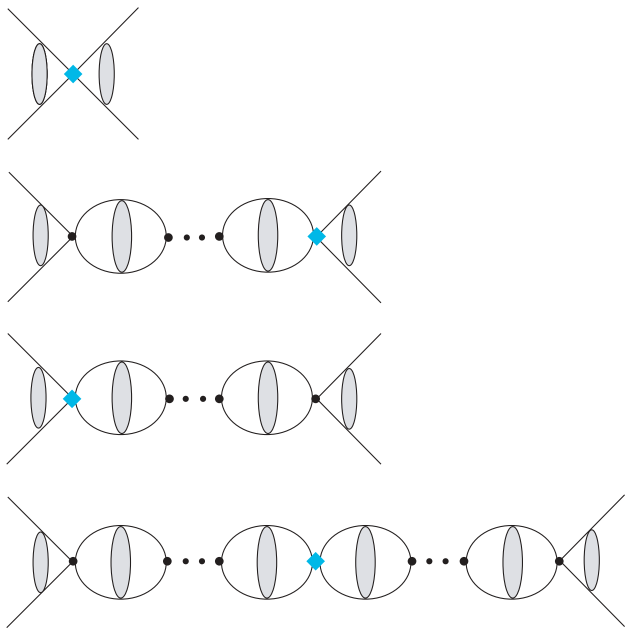

FIG. 4. (Color online) Set 3 of NNLO diagrams. Two-proton contact vertices represented by (blue) diamonds denote strong NNLO potential V_4. See the caption of Fig. 1 for details.

V. REGULARIZATION METHOD AND RENORMALIZATION SCHEMES

In the calculation of the loop functions J_0, J_2, J_{22}, and J_4 in Eqs. (17), (20), (22), and (25), we encounter infinities and employ the dimensional regularization. We also employ the PDS scheme, suggested by Kaplan, Savage, and Wise [8,9], in which one subtracts the poles in $d = 3$ as well as those in $d = 4$ space-time dimensions so that one obtains an expected perturbation series in the expansion of the NN potential in Eq. (10) with a given scale μ of the theory. We may check the convergence radius, e.g., for the C_2 term (relative to the C_0 term) in Eq. (10) and have $\Lambda_{20}(\mu) \equiv \sqrt{C_0(\mu)/C_2(\mu)} = 147(30.6)$ MeV with (without) the PDS terms at $\mu = m_\pi$. Thus a formal convergence of the perturbative series of the NN potential in Eq. (10) is improved thanks to the PDS term, and the theory would be valid up to $p \sim \Lambda_{20} \simeq 140$ MeV, which is the large scale we assumed in the pionless theory.

The loop functions can be decomposed into a finite term and an infinite one, e.g., $J_0 = J_0^{\rm fin} + J_0^{\rm div}$ with $J_0^{\rm fin} = -\frac{\alpha M^2}{4\pi} H(\eta)$ [the definition of the $H(\eta)$ function is given in Appendix B] and

$$J_0^{\rm div} = -\frac{M}{4\pi}\mu + \frac{\alpha M^2}{8\pi}\left[\frac{1}{\epsilon} - 3C_E + 2 + \ln\left(\frac{\pi\mu^2}{\alpha^2 M^2}\right)\right], \tag{26}$$

where $J_0^{\rm div}$ is calculated by the dimensional regularization in $d = 4 - 2\epsilon$ dimensions and the PDS scheme. The first term proportional to the scale μ in the right-hand side of Eq. (26) is the PDS term, and C_E is the Euler's constant mentioned earlier. The scattering amplitudes should be identical after renormalization even if another renormalization scheme such as the off-shell momentum subtraction scheme discussed in Refs. [26,29] is employed. However, $a(\mu)$ and $r(\mu)$ do depend on the renormalization schemes along with the value of the renormalization scale μ. So, to be consistent with KR, we calculate all the loop functions J_i with $i = 0, 2, 22, 4$ and the wave functions ψ_j with $j = 0, 2, 4$ by using the dimensional regularization and the PDS scheme in Appendix B.

The S-wave pp scattering amplitude in terms of the effective range parameters is given by

$$T_{\rm SC}^{l=0} = -\frac{4\pi}{M}\frac{C_\eta^2 e^{2i\sigma_0}}{-\alpha M H(\eta) - \frac{1}{a_C} + \frac{1}{2}r_0 p^2 - P r_0^3 p^4 + \cdots}, \tag{27}$$

and thus one has

$$\begin{aligned} &-\frac{1}{a_C} + \frac{1}{2}r_0 p^2 - P r_0^3 p^4 + \cdots \\ &= \alpha M H(\eta) - \frac{4\pi}{M}C_\eta^2 e^{2i\sigma_0}\frac{1}{T_{\rm SC}^{l=0}} \\ &= \alpha M H(\eta) - \frac{4\pi}{M}\frac{\psi_0^2}{T_{\rm SC}^{(0)}}\left[1 - \frac{T_{\rm SC}^{(2)}}{T_{\rm SC}^{(0)}} - \frac{T_{\rm SC}^{(4)}}{T_{\rm SC}^{(0)}} + \left(\frac{T_{\rm SC}^{(2)}}{T_{\rm SC}^{(0)}}\right)^2 \right. \\ &\quad \left. + \cdots\right]. \end{aligned} \tag{28}$$

Comparing the coefficients of the terms proportional to p^0, p^2, and p^4 in both sides of Eq. (28), we have

$$\begin{aligned} -\frac{1}{a_C} = &-\frac{4\pi}{M}\left\{\frac{1}{C_0} - J_0^{\rm div} + \frac{C_2}{C_0^2}\left[\alpha M\mu + \frac{1}{2}(\alpha M)^2 \right.\right. \\ &\left.\left. + C_0\frac{\pi M}{48}(\alpha M)^2\mu\right] - \left(\frac{1}{2}\frac{C_4}{C_0^2} - \frac{C_2^2}{C_0^3}\right)(\alpha M)^2\mu^2\right\} \\ &+ \mathcal{O}(\alpha^3), \end{aligned} \tag{29}$$

$$\begin{aligned} +\frac{1}{2}r_0 = \frac{4\pi}{M}&\left[\frac{C_2}{C_0^2} - 2\left(\frac{1}{2}\frac{C_4}{C_0^2} + \frac{1}{3}\frac{\tilde{C}_4}{C_0^2} - \frac{C_2^2}{C_0^3}\right)\right. \\ &\left.\times(\alpha M)\mu\right] + \mathcal{O}(\alpha^2), \end{aligned} \tag{30}$$

$$-P r_0^3 = \frac{4\pi}{M}\left(\frac{1}{2}\frac{C_4}{C_0^2} + \frac{1}{2}\frac{\tilde{C}_4}{C_0^2} - \frac{C_2^2}{C_0^3}\right), \tag{31}$$

where we have expanded the right-hand side of Eqs. (29) and (30) in the order of the fine structure constant α and neglected the α^3 (α^2) and higher order terms in Eq. (29) [Eq.(30)]. With three effective range parameters, we cannot determine the four LECs uniquely. There are some arguments which can constrain the values of C_4 and $\tilde{C}_4$. The C_4 contribution in Eq. (29) is of the order of μ^2, and thus the first $\tilde{C}_4$ contribution term is of the lower order of μ than the C_4 term.[5] For this reason, the $\tilde{C}_4$ term is treated as an order higher than the C_4 one [23], and consequently the $\tilde{C}_4$ term does not appear (at NNLO) in Eq. (29). The other argument is based on the offshell-ness of a term proportional to $C_4 - \tilde{C}_4$ [26].[6] In this case, the term proportional to $C_4 - \tilde{C}_4$ is redundant and thus can be removed

[5]Note that μ is regarded as a large scale, i.e., $\mu = m_\pi$.
[6]See footnote 3.

by assuming $C_4 = \tilde{C}_4$. Because both arguments seem to have some grounds, to check the dependency of the results on the values of C_4 and $\tilde{C}_4$ we consider the three cases: (1) $\tilde{C}_4 = 0$ (Ref. [23]), (2) $C_4 = \tilde{C}_4$ (Ref. [26]), and (3) $C_4 = 0$.

In Eq. (29) there is the $J_0^{\rm div}$ term explicitly given in Eq. (26). In the MS scheme used by KR [6,7] one subtracts the infinite term $\frac{\alpha M^2}{8\pi}\frac{1}{\epsilon}$ from $J_0^{\rm div}$. One can use another scheme called the $\overline{\rm MS}$ scheme, in which finite terms are subtracted together with the infinite term so that $\frac{\alpha M^2}{8\pi}[\frac{1}{\epsilon} - C_E + \ln(4\pi)]$ is subtracted. Then we have

$$J_0^{\overline{MS}} = -\frac{M}{4\pi}\mu + \frac{\alpha M^2}{4\pi}\left[\ln\left(\frac{\mu}{2\alpha M}\right) + 1 - C_E\right]. \quad (32)$$

This leads to a significant subtraction scheme dependence in the scattering length $a(\mu)$.

VI. NUMERICAL RESULTS

We may define the strong scattering length and the effective range, respectively, in the zeroth order of α as [7]

$$\frac{1}{a(\mu)} = \frac{4\pi}{M}\frac{1}{C_0(\mu)} + \mu, \qquad \frac{1}{2}r(\mu) = \frac{4\pi}{M}\frac{C_2(\mu)}{C_0^2(\mu)}. \quad (33)$$

Inserting the expressions of $a(\mu)$ and $r(\mu)$ in Eq. (33) into Eqs. (29) and (30), we have

$$\frac{1}{a(\mu)} = \left[\frac{1}{a(\mu)}\right]_{\rm LO} + \left[\frac{1}{a(\mu)}\right]_{\rm NLO} + \left[\frac{1}{a(\mu)}\right]_{\rm NNLO}, \quad (34)$$

$$r(\mu) = r_0 - (\alpha M)\left[D_3 P r_0^3 \mu + D_4 \frac{r_0^2\mu}{\frac{1}{a_C} - \mu}\right], \quad (35)$$

where

$$\left[\frac{1}{a(\mu)}\right]_{\rm LO} = \frac{1}{a_C} + \alpha M\left[\ln\left(\frac{\mu}{2\alpha M}\right) + 1 - C_E\right], \quad (36)$$

$$\left[\frac{1}{a(\mu)}\right]_{\rm NLO} = -\frac{1}{2}\alpha M r_0 \mu - (\alpha M)^2 \times \left[\frac{1}{4}r_0 + \frac{\pi^2}{12}\frac{r_0\mu}{\frac{1}{a_C} - \mu}\right], \quad (37)$$

$$\left[\frac{1}{a(\mu)}\right]_{\rm NNLO} = (\alpha M)^2\left[D_1 P r_0^3 \mu^2 - \frac{D_2 r_0 \mu}{12}\frac{r_0\mu}{\frac{1}{a_C} - \mu}\right], \quad (38)$$

and the term linear in αM in Eq. (35) is the NNLO correction to $r(\mu)$. We have three sets of coefficients, $X_{x(=1,2,3)} = \{D_1, D_2, D_3, D_4\}$, because of the additional constraints imposed on the LECs C_4 and $\tilde{C}_4$ mentioned before Eq. (32). $X_1 = \{1, 0, 4, 0\}$ corresponds to case (1) $\tilde{C}_4 = 0$; $X_2 = \{7/6, 1, 10/3, 1/6\}$ corresponds to case (2) $\tilde{C}_4 = C_4$; and $X_3 = \{4/3, -10, 8/3, 1/3\}$ to case (3) $C_4 = 0$. We use the values of effective range parameters

$$a_C = -7.82 \text{ fm}, \qquad r_0 = 2.78 \text{ fm}, \qquad P \simeq 0.022. \quad (39)$$

We can also have explicit expressions for the LECs $C_0(\mu)$, $C_2(\mu)$, $C_4(\mu)$, and $\tilde{C}_4(\mu)$ from Eqs. (34), (35), and (31) with the constraints for C_4 and $\tilde{C}_4$.

In Fig. 5, we plot our result of the strong scattering length $a(\mu)$ as a function of the scale parameter μ. In the left panel, we plot three curves for the strong scattering length $a(\mu)$ up to LO, NLO, and NNLO with the constraint $\tilde{C}_4 = 0$ [case (1)]. We find that the NLO correction significantly improves the estimation of $a(\mu)$, as shown by KR.

If one looks into the details more closely, however, there is a quantitative difference in the results of LO and NLO between the MS and $\overline{\rm MS}$ schemes. The value of the LO scattering length $a_{\rm LO}(\mu)$ at $\mu = m_\pi$ in the $\overline{\rm MS}$ scheme, which is obtained from Eq. (36), is $a_{\rm LO}^{\overline{MS}}(\mu = m_\pi) = -30.72$ fm. The LO contributions to $a(\mu)$ can be divided into three terms: $1/a_C$, the term proportional to a log function, and the remaining ones proportional to αM. Evaluating each contribution, we obtain $1/a_C = -0.1279$, $\alpha M \ln(\frac{m_\pi}{2\alpha M}) = 0.0807$, and $\alpha M(1 - C_E) = 0.0147$ in units of fm^{-1} in the $\overline{\rm MS}$ scheme. There is a strong cancellation between $1/a_C$ and the log term which has the order of αM. Consequently $1/a(\mu = m_\pi)$ becomes a small value, making its inverse large. In the case of the MS scheme, the cancellation is stronger, having the log term $\alpha M \ln(\frac{\pi m_\pi^2}{\alpha^2 M^2}) = 0.1247$ and $\alpha M(-3C_E + 2)/2 = 0.0047$ in units of fm^{-1}. The cancellation of $1/a_C$ and the terms proportional to αM makes the value of $1/a(\mu = m_\pi)$ two orders of magnitude smaller than $1/a_C$. As a result, one gets an unrealistically huge scattering length, $a_{\rm LO}^{MS}(\mu = m_\pi) = 738.62$ fm. The strong dependence on the renormalization schemes of the LO contribution to $a(\mu)$ makes the EFT result somehow arbitrary.

The NLO contribution, Eq. (37), can be divided into terms linear in αM and those proportional to $(\alpha M)^2$. The term linear in αM is comparable in magnitude with the LO contribution because of the cancellation in LO, as discussed above. More precisely, we have $1/a_{\rm LO}^{\overline{MS}} = -0.0325$ and $-\alpha M r_0 \mu/2 = -0.0343$ in units of fm^{-1}. On the other hand, the numerical value of the contribution proportional to $(\alpha M)^2$ is 0.0015 in units of fm^{-1}, which is about 5% of the terms linear in αM.

The NNLO contribution is very small, as can be seen from the left and right panels in Fig. 5 and in Table I. The reason can be easily found from the expressions for the NNLO terms in Eq. (38). These terms are proportional to $(\alpha M)^2$. We observed in NLO that the $(\alpha M)^2$ term is smaller than the αM order term by an order of magnitude. The magnitude of $(\alpha M)^2$ terms in NNLO ranges from about 20% to 300% of $(\alpha M)^2$ terms in NLO, depending on the choice of the assumptions on C_4 and $\tilde{C}_4$. Consequently, the NNLO correction to $1/a(\mu)$ is about $1 \sim 6\%$ of the contributions up to NLO, depending on the constraints of C_4 and $\tilde{C}_4$.

In Table I we show the estimated values of the strong scattering length $a(\mu)$ and effective range $r(\mu)$ at

TABLE I. Numerical estimations (in units of fm) of scattering length $a(\mu)$ and effective range $r(\mu)$ up to NLO and NNLO without Coulomb effect at $\mu = 140$ MeV.

	NLO	NNLO-1	NNLO-2	NNLO-3
$a(\mu)$	−14.98	−15.11	−15.18	−14.62
$r(\mu)$	—	2.73	2.78	2.82

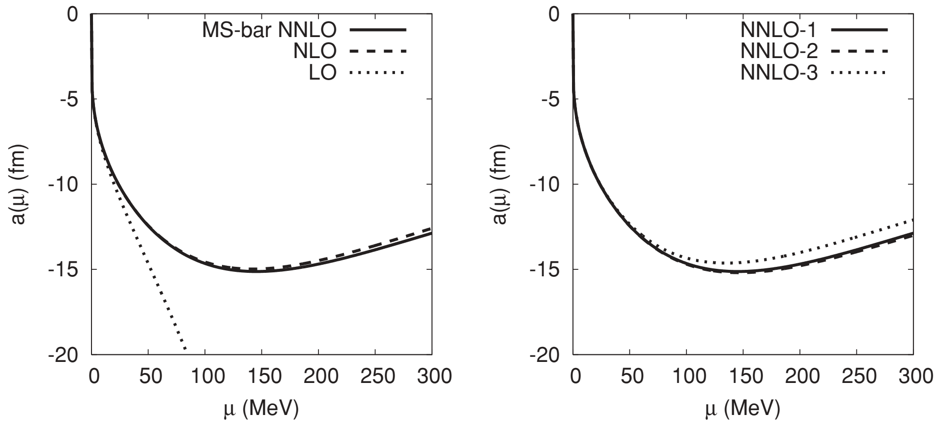

FIG. 5. Strong scattering length $a(\mu)$ in functions of the scale parameter μ. In the left panel, $a(\mu)$ is plotted for up to LO, NLO, and NNLO. In the right panel, $a(\mu)$ calculated up to NNLO are plotted for the three different constraints for C_4 and $\tilde{C}_4$, which are explained in the text.

$\mu = m_\pi$.[7] The NNLO term itself varies by an order of magnitude depending on the choice of the constraints on C_4 and $\tilde{C}_4$. However, as discussed in a previous paragraph, its contribution to $a(\mu)$ is suppressed due to a higher order of αM factor. As a result, the different choice of the constraints on C_4 and $\tilde{C}_4$ affects little the final result, only a few percents at most. The first correction to $r(\mu)$ appears at NNLO and is linear in αM, whereas the NLO correction to $1/a(\mu)$ does in the αM order. Contrary to the case of $1/a(\mu)$ where the αM correction plays a crucial role, the αM contribution to $r(\mu)$ amounts to only about 2% of r_0. Though the αM order corrections to $1/a(\mu)$ and $r(\mu)$ are of the same order of magnitude, the $(\alpha M)^0$ order contribution to $1/a_C$ is smaller than that of r_0 by an order of magnitude. Consequently, we have very contrasting behaviors of $a(\mu)$ and $r(\mu)$.

Thus our results of the strong pp scattering length and effective range up to NNLO, which are estimated by employing the dimensional regularization and the $\overline{\text{MS}}$ and PDS schemes at $\mu = m_\pi$, can be summarized as

$$a(\mu = m_\pi) = -14.9 \pm 0.3 \text{ fm}, \tag{40}$$

$$r(\mu = m_\pi) = 2.78 \pm 0.05 \text{ fm}, \tag{41}$$

where the error bars are estimated by the uncertainties due to the constraints on C_4 and $\tilde{C}_4$, which could play a similar role to that of the model dependence in deducing the values of the strong scattering length a_{pp} and effective range $r_{0,pp}$ in the potential model calculations.

VII. DISCUSSION AND CONCLUSIONS

In this work, we calculated the S-wave pp scattering amplitude up to NNLO in the framework of the pionless EFT. The loop functions were calculated by using the dimensional regularization with the $\overline{\text{MS}}$ and PDS schemes. After fixing the LECs by using the effective range parameters, we estimated the strong scattering length $a(\mu)$ and the strong effective range $r(\mu)$ as functions of μ. The LO contributions to $1/a(\mu)$ are composed of $1/a_C$ and the terms depending on αM arising from the loop diagrams. The smallness of $1/a_C$ makes it comparable in magnitude to the αM terms in the same order. Furthermore, because of the opposite signs of $1/a_C$ and the αM terms, there is a strong cancellation among them and thus it makes the LO result for $1/a(\mu)$ suppressed and sensitive to the renormalization schemes. The NLO correction, expanded in powers of αM, begins with the linear order of αM. The linear αM order correction to $a(\mu)$ is of the same order of magnitude as the αM terms in LO and thus makes the NLO contribution crucial in both the MS and $\overline{\text{MS}}$ schemes. The higher αM order terms in NLO, e.g., the terms proportional to $(\alpha M)^2$, are suppressed to a few percents of the leading contribution, so they can be regarded as perturbative corrections to both $a(\mu)$ and $r(\mu)$. The NNLO terms give us only a fairly minor correction to the results up to NLO. The reason is partly attributed to the additional order counting of the NNLO terms in powers of αM: the αM order corrections in NNLO begin with $(\alpha M)^2$. Similar to the $(\alpha M)^2$ contribution in NLO, the terms in NNLO produce small corrections to the results. In conclusion, we can say that our investigation reveals both bright and shadowy aspects of studying the strong pp scattering length in EFT. Convergence from NLO to NNLO is satisfactory, but the LO and NLO results are significantly dependent on the renormalization schemes.

Though the quantities of the strong scattering length and effective range from the pp scattering could be regarded as physical quantities, it is unlikely that they can be determined unambiguously without the subtraction scheme and renormalization scale dependence within the present framework of EFT. Similar arguments can be found in Refs. [30,31]. Nevertheless, the strong pp scattering length and effective range are important ingredients for better understanding of the isospin nature of the NN interaction. The problem of the strong pp scattering length may have to be approached at various levels, from "first principle calculations" like lattice QCD to more complex systems in which $a(\mu)$ [or equivalently $C_0(\mu)$] plays a nontrivial role.

ACKNOWLEDGMENTS

We thank Yoonbai Kim for a useful comment on our work. S.A. thanks F. Ravndal for communications. S.A. is supported by the Korean Research Foundation and the Korean Federation of Science and Technology Societies Grant funded by the Korean Government (MOEHRD, Basic Research Promotion

[7]We find a minimum point for $a(\mu)$ at $\mu \simeq 2/r_0 \simeq 142$ MeV, which is very close to the pion mass, $\mu = m_\pi$.

Fund): the Brain Pool program (052-1-6) and KRF-2006-311-C00271. The work is in part supported by the Korea Science and Engineering Foundation grant funded by the Korean Government (MOST) (No. M20608520001-07B0852-00110).

APPENDIX A: AMPLITUDES IN NNLO

In this Appendix we present expressions of each of the amplitudes in NNLO in terms of functions $\psi_{0,2,4}$ and $J_{0,2,22,4}$. Detailed calculations of the ψ and J functions are given in Appendix B. From diagram (a) in Fig. 2, we have

$$\begin{aligned} T_{\rm SC}^{(4,a)} &= \langle \psi_{\vec{p}'}^{(-)} | \hat{V}_2 \hat{G}_C^{(+)} \sum_{n=0}^{\infty} (\hat{V}_0 \hat{G}_C^{(+)})^n \hat{V}_0 G_C^{(+)} \hat{V}_2 | \psi_{\vec{p}}^{(+)} \rangle \\ &= \frac{C_0}{1 - C_0 J_0} \int \frac{d^3\vec{q}'}{(2\pi)^3} \langle \psi_{\vec{p}'}^{(-)} | \hat{V}_2 \hat{G}_C^{(+)} | \vec{q}' \rangle \\ &\quad \times \int \frac{d^3\vec{q}}{(2\pi)^3} \langle \vec{q} | \hat{G}_C^{(+)} \hat{V}_2 | \psi_{\vec{p}}^{(+)} \rangle \\ &= \frac{1}{4} \frac{C_0 C_2^2}{1 - C_0 J_0} (\psi_0 J_2 + \psi_2 J_0)^2. \end{aligned} \tag{A1}$$

From diagrams (b) and (c) in Fig. 2, we have

$$\begin{aligned} T_{\rm SC}^{(4,b,c)} &= \langle \psi_{\vec{p}'}^{(-)} | \sum_{n=0}^{\infty} (\hat{V}_0 G_C^{(+)})^n \hat{V}_0 \hat{G}_C^{(+)} \hat{V}_2 \hat{G}_C^{(+)} \\ &\quad \times \sum_{m=0}^{\infty} (\hat{V}_0 G_C^{(+)})^m \hat{V}_0 G_C^{(+)} \hat{V}_2 | \psi_{\vec{p}}^{(+)} \rangle \\ &\quad + \langle \psi_{\vec{p}'}^{(-)} | \hat{V}_2 \hat{G}_C^{(+)} \sum_{n=0}^{\infty} (\hat{V}_0 G_C^{(+)})^n \hat{V}_0 \hat{G}_C^{(+)} \hat{V}_2 \hat{G}_C^{(+)} \\ &\quad \times \sum_{m=0}^{\infty} (\hat{V}_0 G_C^{(+)})^m \hat{V}_0 | \psi_{\vec{p}}^{(+)} \rangle \\ &= \frac{C_0^2 \psi_0}{(1 - C_0 J_0)^2} \int \frac{d^3\vec{q}}{(2\pi)^3} \frac{d^3\vec{q}'}{(2\pi)^3} \langle \vec{q}' | \hat{G}_C^{(+)} \hat{V}_2 \hat{G}_C^{(+)} | \vec{q} \rangle \\ &\quad \times \int \frac{d^3\vec{k}}{(2\pi)^3} [\langle \vec{k} | \hat{G}_C^{(+)} \hat{V}_2 | \psi_{\vec{p}}^{(+)} \rangle + \langle \psi_{\vec{p}'}^{(-)} | \hat{V}_2 \hat{G}_C^{(+)} | \vec{k} \rangle] \\ &= \frac{C_0^2 C_2^2 \psi_0 J_0 J_2}{(1 - C_0 J_0)^2} (\psi_0 J_2 + \psi_2 J_0). \end{aligned} \tag{A2}$$

From diagram (d) in Fig. 2, we have

$$\begin{aligned} T_{\rm SC}^{(4,d)} &= \langle \psi_{\vec{p}'}^{(-)} | \sum_{l=0}^{\infty} (\hat{V}_0 \hat{G}_C^{(+)})^l \hat{V}_0 \hat{G}_C^{(+)} \hat{V}_2 \hat{G}_C^{(+)} \\ &\quad \times \sum_{m=0}^{\infty} (\hat{V}_0 \hat{G}_C^{(+)})^m \hat{V}_0 \hat{G}_C^{(+)} \hat{V}_2 \hat{G}_C^{(+)} \\ &\quad \times \sum_{n=0}^{\infty} (\hat{V}_0 \hat{G}_C^{(+)})^n \hat{V}_0 | \psi_{\vec{p}}^{(+)} \rangle \\ &= \frac{C_0^3 \psi_0^2}{(1 - C_0 J_0)^3} \left[\int \frac{d^3\vec{q}'}{(2\pi)^3} \frac{d^3\vec{q}}{(2\pi)^3} \langle \vec{q}' | \hat{G}_C^{(+)} \hat{V}_2 \hat{G}_C^{(+)} | \vec{q} \rangle \right]^2 \\ &= \frac{C_0^3 C_2^2 \psi_0^2}{(1 - C_0 J_0)^3} J_0^2 J_2^2. \end{aligned} \tag{A3}$$

From diagram (e) in Fig. 3, we have

$$\begin{aligned} T_{\rm SC}^{(4,e)} &= \langle \psi_{\vec{p}'}^{(-)} | \hat{V}_2 \hat{G}_C^{(+)} \hat{V}_2 | \psi_{\vec{p}}^{(+)} \rangle \\ &= \frac{C_2^2}{4} (\psi_0^2 J_{22} + \psi_2^2 J_0 + 2\psi_0 \psi_2 J_2). \end{aligned} \tag{A4}$$

From diagrams (f) and (g) in Fig. 3, we have

$$\begin{aligned} T_{\rm SC}^{(4,f,g)} &= \langle \psi_{\vec{p}'}^{(-)} | \sum_{n=0}^{\infty} (\hat{V}_0 \hat{G}_C^{(+)})^n \hat{V}_0 \hat{G}_C^{(+)} \hat{V}_2 \hat{G}_C^{(+)} \hat{V}_2 | \psi_{\vec{p}}^{(+)} \rangle \\ &\quad + \langle \psi_{\vec{p}'}^{(-)} | \hat{V}_2 \hat{G}_C^{(+)} \hat{V}_2 \hat{G}_C^{(+)} \sum_{n=0}^{\infty} (\hat{V}_0 \hat{G}_C^{(+)})^n \hat{V}_0 | \psi_{\vec{p}}^{(+)} \rangle \\ &= \frac{1}{2} \frac{C_0 C_2^2 \psi_0}{1 - C_0 J_0} (\psi_0 J_2^2 + 2\psi_2 J_0 J_2 + \psi_0 J_0 J_{22}). \end{aligned} \tag{A5}$$

From diagram (h) in Fig. 3, we have

$$\begin{aligned} T_{\rm SC}^{(4,h)} &= \langle \psi_{\vec{p}'}^{(-)} | \sum_{m=0}^{\infty} (\hat{V}_0 \hat{G}_C^{(+)})^m \hat{V}_0 \hat{G}_C^{(+)} \hat{V}_2 \hat{G}_C^{(+)} \hat{V}_2 \hat{G}_C^{(+)} \\ &\quad \times \sum_{n=0}^{\infty} (\hat{V}_0 \hat{G}_C^{(+)})^n \hat{V}_0 | \psi_{\vec{p}}^{(+)} \rangle \\ &= \frac{1}{4} \frac{C_0^2 C_2^2 \psi_0^2}{(1 - C_0 J_0)^2} (3 J_0 J_2^2 + J_0^2 J_{22}). \end{aligned} \tag{A6}$$

From diagram (i) in Fig. 4, we have

$$T_{\rm SC}^{(4,i)} = \langle \psi_{\vec{p}}^{(-)} | \hat{V}_4 | \psi_{\vec{p}}^{(+)} \rangle = \tfrac{1}{2} C_4 \psi_2^2 + \tfrac{1}{2} \tilde{C}_4 \psi_0 \psi_4. \tag{A7}$$

From diagrams (j) and (k) in Fig. 4, we have

$$\begin{aligned} T_{\rm SC}^{(4,j,k)} &= \langle \psi_{\vec{p}'}^{(-)} | \sum_{n=0}^{\infty} (\hat{V}_0 \hat{G}_C^{(+)})^n \hat{V}_0 \hat{G}_C^{(+)} \hat{V}_4 | \psi_{\vec{p}}^{(+)} \rangle \\ &\quad + \langle \psi_{\vec{p}'}^{(-)} | \hat{V}_4 \hat{G}_C^{(+)} \sum_{n=0}^{\infty} (\hat{V}_0 \hat{G}_C^{(+)})^n \hat{V}_0 | \psi_{\vec{p}}^{(+)} \rangle \\ &= \frac{1}{2} \frac{C_0 \psi_0}{1 - C_0 J_0} [2 C_4 \psi_2 J_2 + \tilde{C}_4 (\psi_0 J_4 + \psi_4 J_0)]. \end{aligned} \tag{A8}$$

From diagram (l) in Fig. 4, we have

$$\begin{aligned} T_{\rm SC}^{(4,l)} &= \langle \psi_{\vec{p}'}^{(-)} | \sum_{m=0}^{\infty} (\hat{V}_0 \hat{G}_C^{(+)})^m \hat{V}_0 \hat{G}_C^{(+)} \hat{V}_4 \hat{G}_C^{(+)} \\ &\quad \times \sum_{n=0}^{\infty} (\hat{V}_0 \hat{G}_C^{(+)})^n \hat{V}_0 | \psi_{\vec{p}}^{(+)} \rangle \\ &= \frac{1}{2} \frac{C_0^2 \psi_0^2}{(1 - C_0 J_0)^2} [C_4 J_2^2 + \tilde{C}_4 J_0 J_4]. \end{aligned} \tag{A9}$$

APPENDIX B: LOOP FUNCTIONS

In this Appendix, we present ψ functions (ψ_0, ψ_2, ψ_4) and J functions (J_0, J_2, J_{22}, J_4) employing dimensional regularization and the power divergent regularization scheme [7,8]. We first show the calculations of the ψ_0, ψ_2, and ψ_4 functions in Eqs. (16), (19), and (24).

(i) ψ_0: The Fourier transformation of the Coulomb wave function $\psi_{\vec{p}}^{(\pm)}(\vec{r})$ is

$$\psi_{\vec{p}}^{(\pm)}(\vec{k}) = \int d^3\vec{r}\,\psi_{\vec{p}}^{(\pm)}(\vec{r})\,e^{-i\vec{k}\cdot\vec{r}}, \tag{B1}$$

with

$$\psi_{\vec{p}}^{(\pm)}(\vec{r}) = \sum_{l=0}^{\infty}(2l+1)i^l R_l^{(\pm)}(pr)P_l(\cos\theta), \tag{B2}$$

where $\cos\theta = \hat{p}\cdot\hat{r}$. One has the relation $\vec{k}\cdot\vec{r} = kr[\cos\theta\cos\hat{\theta}+\sin\theta\sin\hat{\theta}\cos(\phi-\hat{\phi})]$, where $\vec{r}$ and $\vec{k}$ are represented by (r,θ,ϕ) and $(k,\hat{\theta},\hat{\phi})$, respectively. Now we choose $\hat{\phi}=0$ and then have

$$\int_0^{2\pi} d\phi\, e^{-ikr\sin\theta\sin\hat{\theta}\cos\phi} = 2\pi J_0(-kr\sin\theta\sin\hat{\theta}), \tag{B3}$$

where J_n is a Bessel function, and we have used Bessel's first integral, $J_n(z) = \frac{1}{2\pi i^n}\int_0^{2\pi} d\phi e^{iz\cos\phi}\,e^{in\phi}$. Using the relations,

$$\int_0^{\pi} d\theta\,\sin\theta\,P_l(\cos\theta)J_0(-kr\sin\theta\sin\hat{\theta})e^{-ikr\cos\theta\cos\hat{\theta}}$$
$$= i^l\sqrt{\frac{2\pi}{-kr}}P_l(\cos\theta)J_{l+\frac{1}{2}}(-kr), \tag{B4}$$

$J_l(-z) = (-1)^l J_l(z)$, and $j_l(z) = \sqrt{\frac{\pi}{2z}}J_{l+\frac{1}{2}}(z)$, where Eq. (B4) is obtained from Eq. (15) in Ref. [32], we have

$$\psi_{\vec{p}}^{(\pm)}(\vec{k}) = 4\pi\sum_{l=0}^{\infty}(2l+1)P_l(\cos\hat{\theta}) \times \int_0^{\infty} dr\,r^2 R_l^{(\pm)}(pr)j_l(kr). \tag{B5}$$

Now we calculate ψ_0 by the dimensional regularization. The angular integration will pick up the $l=0$ part of the wave function; thus, we have

$$\begin{aligned}\psi_0(p) &= \left(\frac{\mu}{2}\right)^{4-d}\int\frac{d^{d-1}\vec{k}}{(2\pi)^{d-1}}\psi_{\vec{p}}^{(+)}(\vec{k})\\ &= 4\pi\left(\frac{\mu}{2}\right)^{4-d}\frac{\Omega_{d-1}}{(2\pi)^{d-1}}\int_0^{\infty}dr\,r^2R_0^{(+)}(pr)\\ &\quad\times\int_0^{\infty}dk\,k^{d-2}j_0(kr)\\ &= (2\pi)^{3/2}\left(\frac{\mu}{2}\right)^{4-d}\frac{\Omega_{d-1}}{(2\pi)^{d-1}}\int_0^{\infty}dr\,r^{3-d}R_0^{(+)}(pr)\\ &\quad\times\int_0^{\infty}d\rho\,\rho^{d-\frac{5}{2}}J_{\frac{1}{2}}(\rho).\end{aligned} \tag{B6}$$

Using the relation $\int_0^{\infty}dt\,t^{\alpha-1}J_\nu(t) = \frac{2^{\alpha-1}}{\Gamma(\frac{1}{2}(2-\alpha+\nu))}\Gamma(\frac{\alpha+\nu}{2})$, we have

$$\int_0^{\infty}d\rho\,\rho^{d-\frac{5}{2}}J_{\frac{1}{2}}(\rho) = 2^{d-\frac{5}{2}}\frac{\Gamma\left(\frac{d-1}{2}\right)}{\Gamma\left(\frac{4-d}{2}\right)}. \tag{B7}$$

Furthermore, from Eq. (6.64) of Ref. [24], we have $R_0^{(+)}(pr) = e^{i\sigma_0}C_\eta\,{}_1F_1(1+i\eta,2;-2ipr)e^{ipr}$, where ${}_1F_1(a;b;z)$ is the confluent hypergeometric function (or Kummer's function of the first kind). Using the relation $\int_0^{\infty}e^{-t}t^{b-1}{}_1F_1(a,c;tz) = \Gamma(b){}_2F_1(a,b,c;z)$, where ${}_2F_1(a,b;c;z)$ is the first hypergeometric function, we have

$$\begin{aligned}&\int_0^{\infty}e^{ipr}r^{3-d}{}_1F_1(1+i\eta,2,-2ipr)\\ &\quad= \Gamma(4-d)(-ip)^{d-4}{}_2F_1(1+i\eta,4-d,2;2),\end{aligned} \tag{B8}$$

and thus

$$\begin{aligned}\psi_0 &= (2\pi)^{3/2}\left(\frac{\mu}{2}\right)^{4-d}\frac{\Omega_{d-1}}{(2\pi)^{d-1}}e^{i\sigma_0}C_\eta\\ &\quad\times\Gamma(4-d)(-ip)^{d-4}{}_2F_1(1+i\eta,4-d,2;2)\\ &\quad\times 2^{d-\frac{5}{2}}\frac{\Gamma\left(\frac{d-1}{2}\right)}{\Gamma\left(\frac{4-d}{2}\right)}.\end{aligned} \tag{B9}$$

There are no poles at $d=3$ and 4 in Eq. (B9). Using the relation ${}_2F_1(1+i\eta,0,2;2)=1$ and $\Omega_d = 2\pi^{d/2}/\Gamma(d/2)$, we have

$$\psi_0 = e^{i\sigma_0}C_\eta. \tag{B10}$$

(ii) ψ_2:

$$\begin{aligned}\psi_2(p) &= \left(\frac{\mu}{2}\right)^{4-d}\int\frac{d^{d-1}\vec{k}}{(2\pi)^{d-1}}\psi_{\vec{p}}^{(+)}(\vec{k})\vec{k}^2\\ &= (2\pi)^{3/2}\left(\frac{\mu}{2}\right)^{4-d}\frac{\Omega_{d-1}}{(2\pi)^{d-1}}\int_0^{\infty}dr\,r^{1-d}R_0^{(+)}(pr)\\ &\quad\times\int_0^{\infty}d\rho\,\rho^{d-\frac{1}{2}}J_{\frac{1}{2}}(\rho)\\ &= (2\pi)^{3/2}\left(\frac{\mu}{2}\right)^{4-d}\frac{\Omega_{d-1}}{(2\pi)^{d-1}}e^{i\sigma_0}C_\eta(-ip)^{d-2}\\ &\quad\times{}_2F_1(1+i\eta,2-d,2;2)2^{d-\frac{3}{2}}\frac{\Gamma\left(\frac{d+1}{2}\right)}{3-d}\frac{\Gamma(4-d)}{\Gamma\left(\frac{4-d}{2}\right)}.\end{aligned} \tag{B11}$$

For $d=4$, we have

$$\psi_2 = e^{i\sigma_0}C_\eta\left(p^2-\frac{1}{2}\alpha^2M^2\right), \tag{B12}$$

where we have used the relation ${}_2F_1(1+i\eta,-2,2,2) = \frac{1}{3}-\frac{2}{3}\eta^2$. For $d=3$, we have

$$\psi_2^{(d=3)} = -e^{i\sigma_0}C_\eta\alpha M\mu\frac{1}{3-d}+\cdots, \tag{B13}$$

where we have used the relation ${}_2F_1(1+i\eta,-1,2;2) = -i\eta$, and thus we have

$$\psi_2 = e^{i\sigma_0}C_\eta\left[p^2-\alpha M\mu-\frac{1}{2}(\alpha M)^2\right]. \tag{B14}$$

(iii) ψ_4:

$$\psi_4 = \left(\frac{\mu}{2}\right)^{4-d}\int\frac{d^{d-1}\vec{k}}{(2\pi)^{d-1}}\psi_{\vec{p}}^{(+)}(\vec{k})\vec{k}^4$$

$$= (2\pi)^{3/2}\left(\frac{\mu}{2}\right)^{4-d}\frac{\Omega_{d-1}}{(2\pi)^{d-1}}\int_0^\infty dr\, r^{-1-d}R_0^{(+)}(pr)$$
$$\times\int_0^\infty d\rho\,\rho^{d+\frac{3}{2}}J_{\frac{1}{2}}(\rho)$$
$$= (2\pi)^{3/2}\left(\frac{\mu}{2}\right)^{4-d}\frac{\Omega_{d-1}}{(2\pi)^{d-1}}e^{i\sigma_0}C_\eta(-ip)^d$$
$$\times\,{}_2F_1(1+i\eta,-d,2;2)\frac{2^{d+\frac{3}{2}}\Gamma\left(\frac{d+3}{2}\right)}{4(1-d)(3-d)}\frac{\Gamma(4-d)}{\Gamma\left(\frac{4-d}{2}\right)}. \tag{B15}$$

For $d=4$, we have

$$\psi_4 = e^{i\sigma_0}C_\eta\left(p^4-\frac{5}{6}\alpha^2M^2p^2+\frac{1}{24}\alpha^4M^4\right), \tag{B16}$$

where we have used the relation ${}_2F_1(1+i\eta,-4,2;2)=\frac{1}{15}(3-10\eta^2+2\eta^4)$. For $d=3$, we have

$$\psi_4^{d=3} = -\frac{4}{3}e^{i\sigma_0}C_\eta\alpha M\mu\left(p^2-\frac{1}{8}\alpha^2M^2\right)\frac{1}{3-d}+\cdots, \tag{B17}$$

where we have used the relation ${}_2F_1(1+i\eta,-3,2;2)=\frac{i}{3}\eta(-2+\eta^2)$. Thus we have

$$\psi_4 = e^{i\sigma_0}C_\eta\left\{p^4-\left[\frac{4}{3}\alpha M\mu+\frac{5}{6}(\alpha M)^2\right]p^2+\frac{1}{6}(\alpha M)^3\mu+\frac{1}{24}(\alpha M)^4\right\}. \tag{B18}$$

Now we calculate loop functions J_0, J_2, J_{22}, and J_4 in Eqs. (17), (20), (22), and (25) by using the results of the ψ functions obtained above.

(iv) J_0: The function $J_0(p)$ is given by [7]

$$J_0(p) = M\int\frac{d^3\vec{l}}{(2\pi)^3}\frac{2\pi\eta(l)}{e^{2\pi\eta(l)}-1}\frac{1}{p^2-l^2+i\epsilon}, \tag{B19}$$

where $l=|\vec{l}|$. We now separate J_0 into two parts as [7]

$$J_0(p) = J_0^{\rm div}+J_0^{\rm fin}, \tag{B20}$$

where

$$J_0^{\rm div} = -M\int\frac{d^3\vec{l}}{(2\pi)^3}\frac{2\pi\eta(l)}{e^{2\pi\eta(l)}-1}\frac{1}{l^2}, \tag{B21}$$
$$J_0^{\rm fin} = M\int\frac{d^3\vec{l}}{(2\pi)^3}\frac{2\pi\eta(l)}{e^{2\pi\eta(l)}-1}\frac{1}{l^2}\frac{p^2}{p^2-l^2+i\epsilon}. \tag{B21}$$

As $J_0^{\rm fin}$ is already calculated in Ref. [7], by changing the parameter $x=2\pi\eta(l)$ and using the relation

$$\int_0^\infty dx\frac{x}{(e^x-1)(x^2+a^2)} = \frac{1}{2}\left[\ln\left(\frac{1}{2\pi}\right)-\frac{\pi}{a}-\psi\left(\frac{1}{2\pi}\right)\right], \tag{B23}$$

where ψ is the logarithmic derivative of the Γ function, we have

$$J_0^{\rm fin} = -\frac{\alpha M^2}{4\pi}H(\eta) = -\frac{\alpha M^2}{4\pi}h(\eta)-C_\eta^2\frac{M}{4\pi}(ip), \tag{B24}$$

where $\eta=\alpha M/(2p)$, $H(\eta)=\psi(i\eta)+\frac{1}{2i\eta}-\ln(i\eta)$, and $h(\eta)=\text{Re }H(\eta)$.

Next we calculate the divergence part $J_0^{\rm div}$ in $d=4-2\epsilon$ dimension as

$$J_0^{\rm div} = -M\left(\frac{\mu}{2}\right)^{4-d}\int\frac{d^{d-1}\vec{q}}{(2\pi)^{d-1}}\frac{2\pi\eta(q)}{e^{2\pi\eta(q)}-1}\frac{1}{q^2}. \tag{B25}$$

Changing the variable $x=2\pi\eta(q)=\pi\alpha M/q$, we have

$$J_0^{\rm div} = -M\left(\frac{\mu}{2}\right)^{4-d}\frac{2\pi^{(d-1)/2}}{(2\pi)^{d-1}\Gamma\left(\frac{d-1}{2}\right)}(\alpha\pi M)^{d-3}\times\int_0^\infty dx\frac{x^{3-d}}{e^x-1}$$
$$= -M\left(\frac{\mu}{2}\right)^{4-d}\frac{2\pi^{(d-1)/2}}{(2\pi)^{d-1}\Gamma\left(\frac{d-1}{2}\right)}(\alpha\pi M)^{d-3}\times\Gamma(4-d)\zeta(4-d), \tag{B26}$$

where we have used the relation $\Omega_d=2\pi^{d/2}/\Gamma(d/2)$, and $\zeta(z)$ is Riemann's ζ function. For $d=4-2\epsilon$, we have

$$J_0^{\rm div} = \frac{\alpha M^2}{8\pi}\left[\frac{1}{\epsilon}-3\gamma+2+\ln\left(\frac{\pi\mu^2}{\alpha^2M^2}\right)\right]. \tag{B27}$$

We also consider the pole for $d=3$, known as the power divergence subtraction (PDS) scheme pole. Using the relation $\lim_{s\to1}[\zeta(s)-\frac{1}{s-1}]=\gamma$, we have the pole at three-dimension

$$J_0^{\rm div} = -\frac{\mu M}{4\pi}\frac{1}{3-d}+\cdots, \tag{B28}$$

and thus we include the PDS counter term and have

$$J_0^{\rm div} = -\frac{M}{4\pi}\mu+\frac{\alpha M^2}{8\pi}\left[\frac{1}{\epsilon}-3\gamma+2+\ln\left(\frac{\pi\mu^2}{\alpha^2M^2}\right)\right]. \tag{B29}$$

(v) J_2:

$$J_2 = \int\frac{d^3\vec{q}}{(2\pi)^3}\frac{d^3\vec{q}\,'}{(2\pi)^3}\vec{q}\,'^2\langle\vec{q}\,'|\hat{G}_C^{(+)}|\vec{q}\rangle$$
$$= M\int\frac{d^3\vec{q}}{(2\pi)^3}\frac{\psi_2(q)\psi_0^*(q)}{\vec{p}^2-\vec{q}^2+i\epsilon}. \tag{B30}$$

Using the result of ψ_2 in Eq. (B14), we get

$$J_2(p) = \left[p^2-\mu\alpha M-\frac{1}{2}(\alpha M)^2\right]J_0(p)-\Delta J_2, \tag{B31}$$

where

$$\Delta J_2 = M\left(\frac{\mu}{2}\right)^{4-d}\int \frac{d^{d-1}\vec{k}}{(2\pi)^{d-1}}\frac{2\pi\eta(k)}{e^{2\pi\eta(k)}-1}$$
$$= M\left(\frac{\mu}{2}\right)^{4-d}\frac{\Omega_{d-1}}{(2\pi)^{d-1}}(\pi\alpha M)^{d-1} \times \Gamma(2-d)\zeta(2-d). \quad \text{(B32)}$$

For $d=4$, we have

$$\Delta J_2 = \frac{1}{4}\pi\alpha^3 M^4\zeta'(-2), \quad \text{(B33)}$$

where $\zeta'(-2) = -0.0304\cdots$. For $d=3$, we obtain

$$\Delta J_2^{(d=3)} = \frac{1}{48}\pi\alpha^2 M^3\mu\frac{1}{3-d}+\cdots, \quad \text{(B34)}$$

and by including the PDS counter term, we have

$$\Delta J_2 = \frac{\pi M}{48}(\alpha M)^2\mu + \frac{\pi M}{4}(\alpha M)^3\zeta'(-2). \quad \text{(B35)}$$

(vi) J_{22}:

$$J_{22} = \int\frac{d^3\vec{q}}{(2\pi)^3}\frac{d^3\vec{q}\,'}{(2\pi)^3}\vec{q}\,'^2\langle\vec{q}\,'|\hat{G}_C^{(+)}|\vec{q}\rangle\vec{q}^{\,2}$$
$$= M\int\frac{d^3\vec{q}}{(2\pi)^3}\frac{\psi_2(q)\psi_2^*(q)}{p^2-q^2+i\epsilon}$$
$$= (p^4-2Ap^2+A^2)J_0 - (p^2-2A)\Delta J_2 - \Delta J_{22}, \quad \text{(B36)}$$

where $A = \mu\alpha M + \frac{1}{2}(\alpha M)^2$, and

$$\Delta J_{22} = M\left(\frac{\mu}{2}\right)^{4-d}\int\frac{d^{d-1}\vec{q}}{(2\pi)^{d-1}}\vec{q}^{\,2}\psi_0(q)\psi_0^*(q)$$
$$= M\left(\frac{\mu}{2}\right)^{4-d}\frac{\Omega_{d-1}}{(2\pi)^{d-1}}(\pi\alpha M)^{d+1}\Gamma(-d)\zeta(-d). \quad \text{(B37)}$$

For $d=4$, we have

$$\Delta J_{22} = \frac{1}{48}\pi^3\alpha^5 M^6\zeta'(-4), \quad \text{(B38)}$$

where $\zeta'(-4) = 0.00798\cdots$. For $d=3$, we get

$$\Delta J_{22}^{(d=3)} = -\frac{1}{2880}\pi^3\alpha^4 M^5\mu\frac{1}{3-d}+\cdots, \quad \text{(B39)}$$

and thus we obtain

$$\Delta J_{22} = -\frac{\pi^3 M}{2880}(\alpha M)^4\mu + \frac{\pi^3 M}{48}(\alpha M)^5\zeta'(-4). \quad \text{(B40)}$$

(vii) J_4:

$$J_4 = \int\frac{d^3\vec{q}}{(2\pi)^3}\frac{d^3\vec{q}\,'}{(2\pi)^3}\vec{q}\,'^4\langle\vec{q}\,'|\hat{G}_C^{(+)}|\vec{q}\rangle$$
$$= M\int\frac{d^3\vec{q}}{(2\pi)^3}\frac{\psi_4(q)\psi_0^*(q)}{p^2-q^2+i\epsilon}. \quad \text{(B41)}$$

Using the relation for ψ_4 in Eq. (B18), we have

$$J_4 = \left\{p^4 - \left[\frac{4}{3}\alpha M\mu + \frac{5}{6}(\alpha M)^2\right]p^2 + \frac{1}{6}(\alpha M)^3\mu + \frac{1}{24}(\alpha M)^4\right\}J_0 - \left[p^2 - \frac{4}{3}\alpha M\mu - \frac{5}{6}(\alpha M)^2\right]\Delta J_2 - \Delta J_{22}. \quad \text{(B42)}$$

[1] S. R. Beane *et al.*, in *At the Frontier of Particle Physics*, edited by M. Shifman (World Scientific, Singapore, 2001), Vol. 1, p. 133.
[2] P. F. Bedaque and U. van Kolck, Annu. Rev. Nucl. Part. Sci. **52**, 339 (2002).
[3] K. Kubodera and T.-S. Park, Annu. Rev. Nucl. Part. Sci. **54**, 19 (2004).
[4] E. Epelbaum, Prog. Part. Nucl. Phys. **57**, 654 (2006).
[5] V. Bernard, Prog. Part. Nucl. Phys. **60**, 82 (2008).
[6] X. Kong and F. Ravndal, Phys. Lett. **B450**, 320 (1999).
[7] X. Kong and F. Ravndal, Nucl. Phys. **A665**, 137 (2000).
[8] D. B. Kaplan, M. J. Savage, and M. B. Wise, Phys. Lett. **B424**, 390 (1998).
[9] D. B. Kaplan, M. J. Savage, and M. B. Wise, Nucl. Phys. **B534**, 329 (1998).
[10] R. B. Wiringa, V. G. J. Stoks, and R. Schiavilla, Phys. Rev. C **51**, 38 (1995).
[11] I. Šlaus, Y. Akaishi, and H. Tanaka, Phys. Rep. **173**, 257 (1989).
[12] G. A. Miller, B. M. K. Nefkens, and I. Šlaus, Phys. Rep. **194**, 1 (1990).
[13] C. R. Howell *et al.*, Phys. Lett. **B444**, 252 (1998).
[14] D. E. González Trotter *et al.*, Phys. Rev. Lett. **83**, 3788 (1999).
[15] V. Huhn, L. Watzold, C. Weber, A. Siepe, W. von Witsch, H. Witala, and W. Glockle, Phys. Rev. Lett. **85**, 1190 (2000).
[16] W. von Witsch, X. Ruan, and H. Witala, Phys. Rev. C **74**, 014001 (2006).
[17] A. Gardestig and D. R. Phillips, Phys. Rev. C **73**, 014002 (2006).
[18] S. Ando and K. Kubodera, Phys. Lett. **B633**, 253 (2006).
[19] S. Albeverio, L. S. Ferreira, F. Gesztesy, R. Hoegh-Krohn, and L. Streit, Phys. Rev. C **29**, 680 (1984).
[20] R. Machleidt, Phys. Rev. C **63**, 024001 (2001).
[21] P. U. Sauer and H. Walliser, J. Phys. G **3**, 1513 (1977); M. Rahman and G. A. Miller, Phys. Rev. C **27**, 917 (1983).
[22] M. Walzl, U.-G. Meißner, and E. Epelbaum, Nucl. Phys. **A693**, 663 (2001).
[23] J.-W. Chen, G. Rupak, and M. J. Savage, Nucl. Phys. **A653**, 386 (1999); M. Butler and J.-W. Chen, Phys. Lett. **B520**, 87 (2001); M. Butler, J.-W. Chen, and X. Kong, Phys. Rev. C **63**, 035501 (2001).
[24] See, e.g., Charles J. Joachain, *Quantum Collision Theory* (North-Holland, Amsterdam, 1975).
[25] H. A. Bethe, Phys. Rev. **76**, 38 (1949).

[26] S. Fleming, T. Mehen, and I. W. Stewart, Nucl. Phys. **A677**, 313 (2000).
[27] L. Durand, III, Phys. Rev. **108**, 1597 (1957); L. Heller, *ibid.* **120**, 627 (1960).
[28] D. Binosi and L. Theussl, Comput. Phys. Commun. **161**, 76 (2004).
[29] J. Gegelia, nucl-th/9802038.
[30] J. Gasser, A. Rusetsky, and I. Scimemi, Eur. Phys. J. C **32**, 97 (2003).
[31] J. Gegelia, Eur. Phys. J. A **19**, 355 (2004).
[32] B. Podolsky and L. Pauling, Phys. Rev. **34** 109 (1929).